QUARTERLY OF APPLIED MATHEMATICS

VOLUME XXXVII January 1980 No. 4

PLANE HARMONIC FUNCTIONS IN THE PRESENCE OF A SURFACE LAYER OF ARBITRARY STIFFNESS*

BY

GEORGE IRENEUS ZAHALAK

Washington University, St. Louis

Abstract. Complex variable techniques are employed to characterize two-dimensional solutions $u(x, y)$ of Laplace's equation which satisfy the boundary condition $[\beta(\partial^2 u/\partial y^2) + (\partial u/\partial x)]_{x=0} = 0$, where β is referred to as the surface-stiffness parameter. Simple closed-form singular solutions are derived which satisfy this boundary condition and represent source and dislocation singularities. The former is used to synthesize the field generated by a small inclusion of arbitrary shape on which $u = 1$, in the presence of a boundary at $y = 0$ on which $u = 0$. At points not near the inclusion the field has the form of a function of position and surface stiffness multiplied by a strength factor which depends on the size and shape of the inclusion and the surface stiffness. Detailed calculations are presented for two extreme shapes of inclusions—a shallow, wide inclusion on the surface and a deep, narrow inclusion penetrating below the surface—which exhibit the relation between the field near the inclusion and the distant field, and show explicitly the dependence of the strength factor on surface stiffness and inclusion size and shape. The nature and strength of the singularities at the tips of the inclusions are also examined and it is found that a tip singularity at the surface changes character as the surface stiffness varies.

Introduction. There exists an important class of physical problems which requires the determination of a function $u(x, y)$ satisfying Laplace's equation in a plane region and also satisfying a boundary condition of the form

$$\beta(\partial^2 u/\partial s^2) + (\partial u/\partial n) = 0 \tag{1}$$

on one or more rectilinear boundaries of that region, where s and n denote respectively the directions parallel and normal to the boundary and β is a real number which can assume any value between zero and infinity. For example, this problem is of central importance in that branch of surface chemistry which deals with the measurement of the "surface viscosity" of molecular monolayers and bilayers [1]. Fig. 1 illustrates the typical physical situation. A cylindrical viscometer is filled with a substrate liquid, usually water, up to a level $x = 0$ and a thin layer of the substance under investigation is spread on this surface. A circular disk or knife-edge is placed in contact with the surface and caused to rotate at constant angular velocity: the cross-section of this perturbing body appears as the shaded region in Fig. 1, and the rigid wall of the viscometer appears as the boundary at $y = 0$. If the radius of the viscometer is large compared to the distance between the wall

* Received December 1, 1978. The author is grateful to Dr. Hiroshi Tada for his helpful comments on this paper.

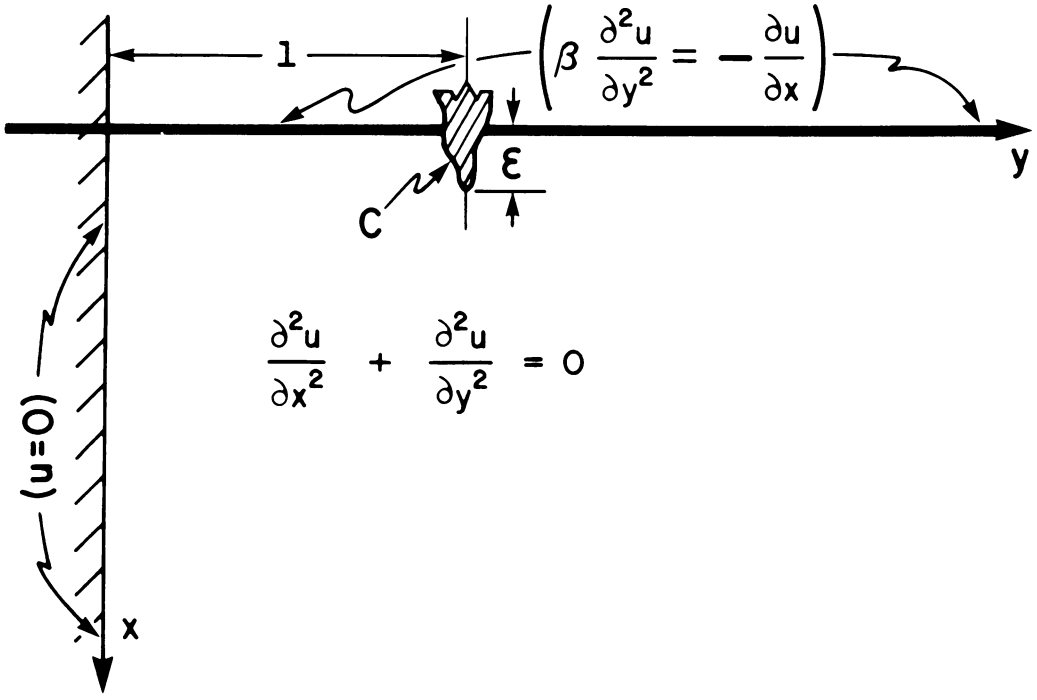

FIG. 1. Geometry of the problem.

and the knife-edge, it is appropriate to approximate the true cylindrical geometry of the viscometer by plane geometry. The surface viscosity—that is, the ratio of shear force per unit length of the layer to the velocity gradient on the surface—can be calculated from measurements of the surface velocity distribution induced by the rotating knife-edge. In order to interpret these measurements correctly one must solve for the circumferential velocity $u(x, y)$ of the fluid in the viscometer. The function u satisfies Laplace's equation for $x > 0$, and for surface layers exhibiting Newtonian surface viscosity it satisfies a boundary condition of the form (1) above, where β is the ratio of the surface viscosity of the layer to the viscosity of the bulk substrate liquid.

In addition to surface viscometry, there are many other physical situations which lead to a mathematically identical problem. Thus static antiplane-strain problems in the theory of elasticity involve solutions of Laplace's equation subject to Eq. (1) if the elastic solid has a plane boundary to which a thin layer of a different material has been bonded (see, for example [2]). In this application u represents the displacement of points perpendicular to the (x, y) plane and β represents the ratio of the shear stiffness of the surface layer to the shear stiffness of the bulk solid. Other applications of the same problem arise in heat conduction, electricity, etc. Because of its wide range of application it seems preferable to discuss this problem in general terms rather than in the context of a particular physical situation. However, I have taken the liberty of referring to the parameter β as the "stiffness" of the surface layer, a term which describes its physical import in the elastostatic problem. Also the region which is shaded in Fig. 1, on the boundary of which the harmonic function u is required to assume a constant value, will be referred to as the "inclusion".

Due to its importance in surface viscometry several analyses of the surface layer prob-

lem have appeared in the surface chemistry literature [3, 4]. Most of these have treated the problem in cylindrical geometry, and the resulting mathematical complications have necessitated a largely numerical treatment of the field generated by a surface inclusion [4]. In particular, there does not appear to be any detailed discussion of the fields generated by inclusions of various shapes which penetrate below the surface. If the problem is restricted to plane geometry then the powerful techniques of complex variable theory permit a comparatively simple and largely analytical discussion of the character of the solutions and their dependence on inclusion geometry and surface layer stiffness. To this end closed-form singular solutions to Laplace's equation satisfying the surface boundary condition Eq. (1) will be derived below, and these will be used to characterize the field produced by a small inclusion on which u = const. in the presence of the surface layer and a boundary on which $u = 0$. Particular attention will be focused on the form of the solution at points not close to the inclusion (the outer field), on the relation between this outer field and the inner field near the inclusion, and also on the form of the singularities at sharp tips of the inclusion.

Mathematical formulation. The geometry of the problem is shown in Fig. 1. We seek a function $u(x, y)$ satisfying the following for $0 < \beta < \infty$:

$$(\partial^2 u/\partial x^2) + (\partial^2 u/\partial y^2) = 0 \quad \text{for } x > 0 \text{ and } y > 0, \text{ and } (x, y) \text{ outside } C, \tag{1}$$

$$u = 0 \quad \text{on} \quad y = 0, \tag{2}$$

$$u = 1 \quad \text{on} \quad C, \tag{3}$$

$$u \to 0 \quad \text{as} \quad r = (x^2 + y^2)^{1/2} \to \infty, \tag{4}$$

$$\beta(\partial^2 u/\partial y^2) + (\partial u/\partial x), = 0 \quad \text{on } x = 0, \text{ outside } C. \tag{5}$$

In the sequel it will be assumed that the characteristic dimension ϵ of the inclusion bounded by C is small.

Singular solutions. The solution to the problem posed above can be synthesized by finding a Green's function associated with an isolated source located at an arbitrary point within the region of interest, and then distributing such sources over the curve C appropriately to satisfy the boundary condition (3). This is accomplished most easily via complex variable techniques. For the unbounded plane the Green's function is well known to be

$$g(x, y, x', y') = \text{Re } \{\log(z - z')\}$$

where $z = x + iy$ and $z' = x' + iy'$ locate respectively the field and source points, and Re denotes the real part of its argument. Therefore we seek first a function $g_1(x, y, x', y'; \beta)$ which for fixed x', y' and β (1) satisfies Laplace's equation in $x > 0$, $-\infty < y < \infty$, (2) has a logarithmic singularity at $z = z'$, (3) has a vanishing gradient at infinity, and finally (4) satisfies the boundary condition Eq. (5) on $x = 0$. Let

$$G_1(z, z'; \beta) = g_1(x, y, x', y'; \beta) + ih_1(x, y, x', y'; \beta).$$

The boundary condition Eq. (5) can be re-stated in complex variable terms as

$$\text{Re} \left\{ \beta \frac{d^2 G_1}{dz^2} - \frac{dG_1}{dz} \right\} = 0 \quad \text{on} \quad x = 0. \tag{6}$$

As $z \to z'$ we require that $G \sim \log (z - z')$, and therefore

$$\left\{\beta \frac{d^2G_1}{dz^2} - \frac{dG_1}{dz}\right\} \sim -\frac{\beta}{(z-z')^2} - \frac{1}{z-z'} \quad \text{as} \quad z \to z'.$$

Boundary condition (6) can be satisfied by superposition of image singularities. Thus we let

$$\beta \frac{d^2G_1}{dz^2} - \frac{dG_1}{dz} = \beta \left\{\frac{1}{(z+z'^*)^2} - \frac{1}{(z-z')^2}\right\} - \left\{\frac{1}{z+z'^*} + \frac{1}{z-z'}\right\}, \tag{7}$$

where * denotes a complex conjugate.

This equation is easily integrated to yield

$$G_1(z, z'; \beta) = \log \{(z-z')(z+z'^*)\} + 2 \exp\left(\frac{z+z'^*}{\beta}\right) E_1\left(\frac{z+z'^*}{\beta}\right), \tag{8}$$

where $E_1(z)$ is the exponential integral function of complex argument

$$E_1(z) = \int_z^\infty (e^{-t}/t)\, dt.$$

The values and properties of this function are listed extensively in [5]. It has a logarithmic singularity at the origin and branch points there and at infinity. The conventional branch cut is taken along the negative x axis and $E_1(z)$ is analytic everywhere off this cut.

The real part of G_1 is the Green's function for a half-plane bounded by a surface layer. It is indeed harmonic for $y > 0$ except at the source point where it has a simple logarithmic singularity, has a vanishing gradient at infinity, and satisfies Eq. (5). In the following E_1 invariably appears multiplied by the exponential, so for the sake of notational convenience we will define the function

$$Expei(z) = \exp(z) E_1(z). \tag{9}$$

The asymptotic expansions of $Expei(z)$ are [5]

$$\begin{aligned} Expei(z) &= z^{-1} - z^{-2} + \cdots \quad \text{as} \quad z \to \infty \\ &= -\log(z) - \gamma - z \log(z) + \cdots \quad \text{as} \quad z \to 0 \end{aligned} \tag{10}$$

where γ is Euler's constant 0.57721 $\cdots$. Thus the effect of the surface layer is confined to the second term of Eq. 8, and vanishes as $\beta \to 0$. On the other hand, as $\beta \to \infty$ the first and second terms combine to give

$$G_1(z, z'; \beta) = 2(\log \beta - \gamma) + \log\left(\frac{z-z'}{z+z'^*}\right) - 2\left(\frac{z+z'^*}{\beta}\right) \log\left(\frac{z+z'^*}{\beta}\right) + \cdots \tag{11}$$

at any finite z. Nevertheless, even for large β, G_1 still approaches 2 log (z) at large distances from the source point. Fig. 2 shows the equipotentials (we will refer to the level curves of Re $\{G_1\}$ or u as equipotentials) for a source at (1, 0) and for small and large β. At low values of β the equipotentials are normal to the surface $((\partial g_1/\partial x) = 0)$, while at high values of β the surface coincides approximately with an equipotential (g_1 = const., $(\partial^2 g_1/\partial y^2) = 0$) at least for points not too distant from the source point. In the immediate vicinity of the source point the equipotentials remain concentric circles characteristic of the simple source singularity. Thus the Green's function (8) contains the essential properties of the solution for arbitrary β, and these will persist when sources are distributed to satisfy the boundary condition on the inclusion.

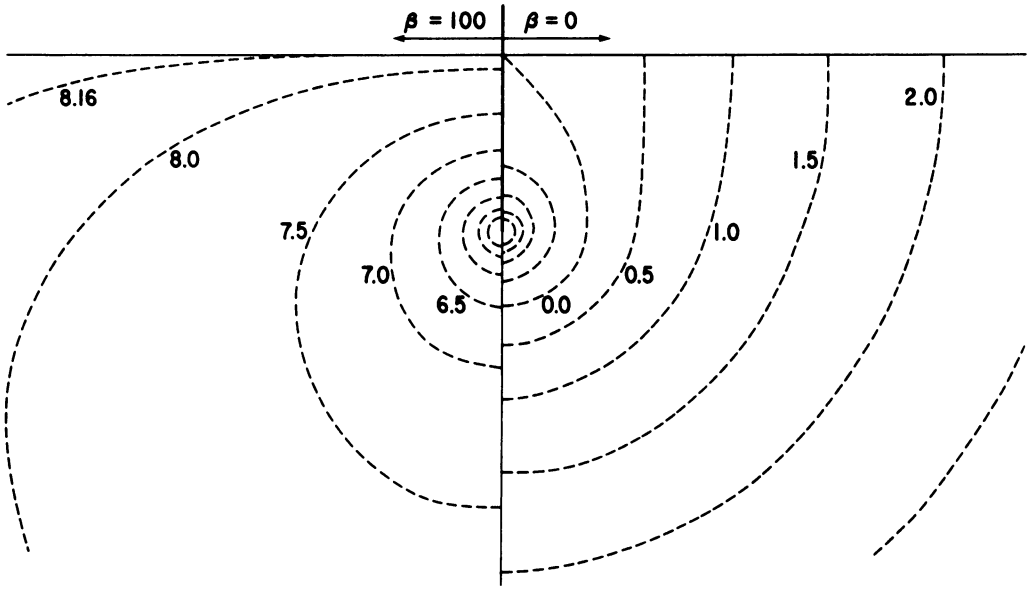

FIG. 2. Equipotentials of the Green's (source) function for low and high surface stiffness.

By an approach similar to the one which was used to arrive at Eq. (8) it is possible to construct an equally simple singular solution to represent a "screw dislocation" in the presence of a surface layer. The complex potential in this case is

$$G_2(z, z'; \beta) = i\left\{\log\left(\frac{z - z'}{z + z'^*}\right) - 2\,Expei\left(\frac{z + z'^*}{\beta}\right)\right\} \tag{11a}$$

and the real part of G_2 represents in the elastostatic antiplane-strain problem the displacement field associated with a screw dislocation located at z' when a stiff surface layer is bonded to the plane $x = 0$. For $x > 0$, G_2 is an analytic function of z everywhere off a branch cut connecting the points z' and z'^*, and on this branch cut Re $\{G_2\}$ changes discontinuously by 2π. Further, G_2 satisfies the surface boundary condition Eq. (6) for arbitrary values of the surface stiffness, and vanishes at infinity. Again the effect of surface stiffness is confined to the second term of Eq. (11*a*) and this term vanishes as $\beta \to 0$. Singularities of this type can be used to synthesize the fields associated with cracks in elastic bodies [6], but this application will not be developed further in this paper.

Before proceeding to a formal solution for inclusions with various shapes, we require the Green's function satisfying the boundary condition Re $\{G\} = 0$ on $y = 0$. This is easily obtained from G_1 by the method of images. Thus

$$\begin{aligned} G(z, z'; \beta) &= G_1(z, z'; \beta) - G_1(z, z'^*; \beta) \\ &= \log\left\{\frac{(z - z')(z + z'^*)}{(z + z')(z - z'^*)}\right\} + 2\left\{Expei\left(\frac{z + z'^*}{\beta}\right) - Expei\left(\frac{z + z'}{\beta}\right)\right\} \end{aligned} \tag{12}$$

and this singular solution satisfies all the conditions of the problem except Eq. (3).

Integral equation for small inclusion of arbitrary shape. Suppose now that an inclusion of characteristic size ϵ bounded by a curve C exists in the vicinity of $z = i$, and $u(x, y)$ must assume the value 1 on C. We can write a formal solution to the problem as a

source distribution over C. Define

$$F(z; \beta, \epsilon) = u(x, y; \beta, \epsilon) + iv(x, y; \beta, \epsilon). \tag{13}$$

Then

$$F(z; \beta, \epsilon) = \int_{C(\epsilon)} G[z, z'(s); \beta] f(s; \beta, \epsilon)\, ds \tag{14}$$

where the real variable s measures arc length along C and $f(s)$ is a real-valued source-density function which must be chosen to satisfy the integral equation

$$\mathrm{Re}\{F(z; \beta, \epsilon)\} = 1 \qquad \text{for } z \text{ on } C. \tag{15}$$

If no restrictions are placed on the size or shape of the inclusion, then the solution may be found numerically, for example by the method outlined in the Appendix. We shall, however, in the remainder of this paper assume that the characteristic dimension of the inclusion satisfies the condition

$$\epsilon \ll 1.$$

In other words, we will seek the leading term of an asymptotic expansion of the solution as $\epsilon \to 0$. In fact, two expansions are required: an "outer expansion" valid when z is not close to the inclusion, and an "inner expansion" valid when it is [7]. These may be extracted from Eq. (12) by introducing the "inner" variables

$$\zeta = \epsilon^{-1}(z - i) = \xi + i\eta \qquad \text{and} \qquad \zeta' = \epsilon^{-1}(z' - i) = \xi' + i\eta'. \tag{16}$$

The one-term outer expansion is obtained by substituting for z' in Eq. (14) its expression in terms of ζ' and taking the limit as $\epsilon \to 0$ with z and ζ' held fixed. In this limit

$$G = G_0(z; \beta) + \cdots \tag{17}$$

where

$$G_0(z; \beta) = 2\left\{\log\left(\frac{z - i}{z + i}\right) + Expei\left(\frac{z - i}{\beta}\right) - Expei\left(\frac{z + i}{\beta}\right)\right\}, \tag{18}$$

so that

$$F(z; \beta, \epsilon) = q(\beta, \epsilon) G_0(z; \beta) + \cdots, \tag{19}$$

where

$$q(\beta, \epsilon) = \int_C f_0'(s'; \beta, \epsilon)\, ds' \tag{20}$$

with $s' = \epsilon^{-1}s$ and

$$f(s; \beta, \epsilon) = \epsilon^{-1} f'(\epsilon s'; \beta, \epsilon) = \epsilon^{-1} f_0'(s'; \beta, \epsilon) + \cdots. \tag{21}$$

The function $\epsilon^{-1} f_0'(s'; \beta, \epsilon)$ is the leading term of the asymptotic expansion of f as $\epsilon \to 0$, and this expansion is assumed uniformly valid in β.

Conversely, the one-term inner expansion is obtained by replacing both z and z' in Eq. (14) by their expressions in terms of ζ, ζ' and ϵ, and taking the limit as $\epsilon \to 0$ with ζ and ζ' fixed. This yields

$$F(\zeta; \beta, \epsilon) = \int_C G'(\zeta, \zeta'; \beta, \epsilon) f_0'(s'; \beta, \epsilon)\, ds' \tag{22}$$

where

$$G'(\zeta, \zeta'; \beta, \epsilon) = \log\{(\zeta - \zeta')(\zeta + \zeta'^*)\} + 2\,Expei\left(\frac{\zeta + \zeta'^*}{\beta/\epsilon}\right) + 2\{\log(\epsilon) - \log(2i) - Expei(2i/\beta)\}. \tag{23}$$

The first-order source density is found by solving the integral equation (15), which may be written as

$$\mathrm{Re}\left\{\int_C G'(\zeta, \zeta'; \beta, \epsilon) f_0'(\zeta'; \beta, \epsilon) e^{-i\phi} d\zeta'\right\} = 1 \qquad \text{for } \zeta \text{ on } C \tag{24}$$

where ϕ is the angle of inclination of the tangent to C with respect to the ξ axis.

A straightforward numerical scheme for solving this equation for arbitary C is outlined in the Appendix. However, progress can be made analytically if we restrict consideration to two extreme shapes of inclusion—a wide, shallow inclusion just touching the surface, and a deep narrow inclusion penetrating below the surface. An analysis of these two cases will reveal the essential features of the fields associated with inclusions of arbitrary shape. For purposes of reference these two extreme shapes will be called respectively the "shallow, wide inclusion" (SWI) and the "deep, narrow inclusion" (DNI). The solutions in these two cases, particularly their behavior for small and large β, will be examined in detail below.

For future reference we list the behavior of G' as (β/ϵ) becomes large or small. Thus

$$G'(\zeta, \zeta'; \beta, \epsilon) = \log\{(\zeta - \zeta')(\zeta + \zeta'^*)\} + 2\{\log(\epsilon) - \log(2i)\} + \cdots \text{ as } (\beta/\epsilon) \to 0 \tag{25}$$

and

$$G'(\zeta, \zeta'; \beta, \epsilon) = \Gamma(\beta) + \log\left(\frac{\zeta - \zeta'}{\zeta + \zeta'^*}\right) - 2\left(\frac{\zeta + \zeta'^*}{\beta/\epsilon}\right)\log\left(\frac{\zeta + \zeta'^*}{\beta/\epsilon}\right) + \cdots \text{ as } (\beta/\epsilon) \to \infty \tag{26}$$

where

$$\Gamma(\beta) = 2\{\log(\beta) - \gamma - \log(2i) - Expei(2i/\beta)\}. \tag{27}$$

Source density for the SWI as $\beta \to 0$ or ∞. In this case the boundary of the inclusion is taken as

$$C: x = 0, \qquad -\epsilon < y - 1 < \epsilon. \tag{28}$$

Further, we have $\zeta'^* = -\zeta' = -i\eta'$, and $\phi = \pi/2$ so that Eq. (24) becomes

$$\mathrm{Re}\left\{-i\int_{-i}^{i} G'(\zeta, \zeta'; \beta, \epsilon) f_0'(\zeta'; \beta, \epsilon)\, d\zeta'\right\} = 1 \qquad \text{for } \zeta = i\eta, \quad |\eta| < 1. \tag{29}$$

In the limit as $\beta \to 0$, Eq. (25) shows that Eq. (29) degenerates to

$$2\int_{-1}^{1} \{\log|\eta - \eta'| + \log(\epsilon/2)\} f_0'(\eta'; \beta, \epsilon)\, d\eta' = 1 \qquad \text{for } |\eta| < 1. \tag{30}$$

Neglecting the higher-order terms in the expansion of G', Eq. (30) can be solved readily by well-known complex variable techniques [8] to yield the limiting form of the source density as $(\beta/\epsilon) \to 0$. Thus we find

$$f_0'(\eta'; \beta, \epsilon) = \{2\pi \log(\epsilon/4)(1 - \eta^2)^{1/2}\}^{-1} + \cdots \qquad \text{as } (\beta/\epsilon) \to 0. \tag{31}$$

On the other hand, as $(\beta/\epsilon) \to \infty$, G' has the expansion of Eq. (26), but if the source point ζ' is on the surface $\xi = 0$ the real part of the second term of Eq. (26) vanishes and we must solve

$$\mathrm{Re}\left\{\int_{-1}^{1}\left[\Gamma(\beta) - 2\,\frac{i\eta - i\eta'}{\beta/\epsilon}\log\frac{i\eta - i\eta'}{\beta/\epsilon}\right]f_0'(\eta';\beta,\epsilon)\,d\eta'\right\} = 1 \qquad \text{for } |\eta| < 1. \tag{32}$$

The solution to Eq. (32) can be found by inspection to be two delta functions, one located at each end of the interval. The solution is

$$f_0'(\eta;\beta,\epsilon) = \frac{\delta(\eta-1)+\delta(\eta+1)}{2[\pi(\epsilon/\beta) + \mathrm{Re}\{\Gamma(\beta)\}]} + \cdots \qquad \text{as } (\beta/\epsilon)\to\infty. \tag{33}$$

Thus in the limit of large β the source density approaches a distribution rather than a classical function.

Source density for the DNI as $\beta \to 0$ and ∞. For the deep, narrow inclusion we take

$$C1{:}10 < x < \epsilon, \qquad y = 0. \tag{34}$$

In this case $\zeta'^* = \zeta' = \xi'$ and $\phi = 0$ so that Eq. (24) becomes

$$\mathrm{Re}\left\{\int_0^1 G'(\zeta,\zeta';\beta,\epsilon)f_0'(\zeta';\beta,\epsilon)d\zeta'\right\} = 1 \qquad \text{for } \zeta = \xi,\ 0 < \xi < 1. \tag{35}$$

As $(\beta/\epsilon) \to 0$ Eq. (35) degenerates to

$$\int_0^1 \{\log|\xi^2 - \xi'^2| + 2\log(\epsilon/2)\}\,f_0'(\xi';\beta,\epsilon)\,d\xi = 1 \qquad \text{for } 0 < \xi < 1 \tag{36}$$

which can again be solved by standard techniques to yield

$$f_0'(\xi;\beta,\epsilon) = \{\pi\log(\epsilon/4)(1-\xi^2)^{1/2}\}^{-1} + \cdots \qquad \text{as } (\beta/\epsilon)\to 0. \tag{37}$$

For $\beta \to \infty$ the situation is somewhat more subtle than it was for the wide, shallow inclusion. In the present case the real part of the second term of Eq. (26) does not vanish but in fact dominates the third term except at points near $\zeta' = 0$. Motivated by the behavior of the source density as $\beta \to \infty$ in the case of the SWI, we postulate an expansion of the form

$$f(\zeta';\beta,\epsilon) = \beta A(\epsilon)\,\delta(\zeta') + \log(\beta) f_{01}'(\zeta';\epsilon) + o(\log(\beta)) \qquad \text{as } \beta\to\infty. \tag{38}$$

Note that this expansion is for $\beta \to \infty$ with ϵ held fixed, not simply for $(\beta/\epsilon) \to \infty$ as in the case of the SWI. The symbol $o(\log(\beta))$ has the conventional meaning of a function the ratio of which to $\log(\beta)$ vanishes as $\beta \to \infty$. If the expansion of Eq. (38) is inserted into Eq. (35) and the terms are ordered in β, the following results

$$\mathrm{Re}\left\{4iA\log(2i/\beta) + \log(\beta)\left[2\zeta\epsilon A + \int_0^1 \log\left(\frac{\zeta-\zeta'}{\zeta+\zeta'}\right)f_{01}'(\zeta';\epsilon)\,d\zeta'\right] + o(\log(\beta))\right\} = 1 \qquad \text{for } 0 < \zeta < 1. \tag{39}$$

As $\beta \to \infty$ this gives rise to the sequence of problems

$$-2\pi A = 1, \qquad \int_0^1 \log\left|\frac{\xi-\xi'}{\xi+\xi'}\right| f_{01}'(\xi';\epsilon)\,d\xi' + 2\epsilon A\xi = 0, \ \cdots. \tag{40}$$

Thus the first problem yields $A = -(1/2\pi)$, while the integral equation of the second problem can be solved to give

$$f_{01}'(\xi; \epsilon) = -(\epsilon/\pi^2)\xi(1 - \xi^2)^{-1/2}, \tag{41}$$

so that a two-term expansion of the source density for the NDI is

$$f_0'(\xi; \beta, \epsilon) = -(\beta/2\pi)\,\delta(\xi) - (\epsilon/\pi^2)\log(\beta)\xi(1 - \xi^2)^{1/2} + \cdots \qquad \text{as } \beta \to \infty. \tag{42}$$

The limiting forms of the source distributions for the SWI and the DNI, Eqs. (31), (33), (37), and (42), can now be inserted into Eqs. (20) and (22) to compute the limiting forms of $q(\beta, \epsilon)$ and the inner complex potential $F(\zeta; \beta, \epsilon)$. The results of the analysis presented in this and the preceding section are summarized in Table I.

Intermediate values of β. To bridge the gap between small and large values of β, the source density function f_0' was determined by solving Eq. (24) numerically, using the scheme presented in the Appendix. Some numerical approximations to the source distribution for the NDI are shown in Fig. 3 for several values of β, and these confirm that as $\beta \to \infty$ the source strength near the origin becomes large while maintaining an inverse square-root singularity at $\xi = 1$. The quantity of primary interest in these calculations is the magnitude of $q(\beta, \epsilon)$ which determines the strength of the outer field. In Fig. 4 the values of $q(\epsilon, \beta)$ for both the SWI and the NDI are displayed as a function of β for several values of the characteristic dimension of the inclusion ϵ. The asymptotic limits for small and large β are shown in solid lines and the numerically computed intermediate values are shown in dashed lines. With the definitions of ϵ we have chosen, $q(\beta, \epsilon)$ approaches the value $(2 \log(\epsilon/4))^{-1}$ as $\beta \to 0$ for both the SWI and the NDI, whereas for large β, $q(\beta, \epsilon)$ approaches $-(\beta/2\pi)$ in both cases. Note that in the case of the SWI, $q(\beta, \epsilon)$ approaches $[\mathrm{Re}\,\{\Gamma(\beta)\}]^{-1}$ when (β/ϵ) is large, even if β itself is not large.

Summary of results for the SWI and the NDI. Eq. (19), together with the results presented in Fig. 4 and Table I, provides a comprehensive description of the behavior of the solution to the problem posed in Eqs. (1) through (5) as β varies from zero to infinity. Fig. 5 shows the variation of the solution near the SWI as β increases, and Fig. 6 exhibits the same information for the NDI. Thus in each case as β becomes large the equipotentials near the surface approach straight lines with a slope that decreases with decreasing ϵ. The tips of the inclusions are singular points for all values of β, but whereas the tip singularity of the NDI retains its square-root character and merely changes its strength as β varies from zero to infinity, the tip singularity for the SWI actually changes character from a square-root to a logarithmic behavior (see Table I).

At points not too close to the inclusion the solution is given by the outer field, Eq. 19. The variation of u on the surface $x = 0$ is shown in Fig. 7, for both the SWI and the NDI and several values of β. Both at low and at high β the curves for both types of inclusions coalesce, but for intermediate values of β differences become evident. Note that as $\beta \to \infty$, u approaches a simple linear variation between $y = 0$ and $y = 1$, and remains constant for $y > 1$.

Discussion. This paper has attempted a reasonably comprehensive discussion of the behavior of plane harmonic functions in the presence of a surface layer of arbitrary stiffness and a small inclusion on the boundary of which the functions assume a constant

TABLE I. Asymptotic behavior of the solutions as $\beta \to 0$ or ∞.

Configuration	Limit	Source Density $f_0'(\xi;\beta,\varepsilon)$	Complex Potential* $F(\zeta;\beta,\varepsilon)$	Outer Field Strength $q(\beta,\varepsilon)$
SWI	$\left(\frac{\beta}{\epsilon}\right) \to 0$	$\{2\pi\log(\varepsilon/4)(1-\xi^2)^{1/2}\}^{-1}$	$1 + \{\log(\varepsilon/4)\}^{-1}\{\text{Arc Sinh}(\zeta)\}$	$\{2\log(\varepsilon/4)\}^{-1}$
SWI	$\left(\frac{\beta}{\epsilon}\right) \to \infty$	$\frac{\delta(\xi-1)+\delta(\xi+1)}{2\{\text{Re}\Gamma(\beta)+\pi(\varepsilon/\beta)\}}$	$\{\text{Re}\Gamma(\beta)+(\varepsilon/\beta)\}^{-1}\{\Gamma(\beta) - (\varepsilon/\beta)[(\zeta-\text{i})\log(\zeta-\text{i}) + (\zeta+\text{i})\log(\zeta+\text{i})] - 2\zeta(\varepsilon/\beta)\log(\varepsilon/\beta)\}$	$\{\text{Re}\Gamma(\beta)+(\pi)(\varepsilon/\beta)\}^{-1}$**
DNI	$\left(\frac{\beta}{\epsilon}\right) \to 0$	$\{\pi\log(\varepsilon/4)(1-\zeta^2)^{-1/2}$	$1 + \{\log(\varepsilon/4)\}^{-1}\{\text{Arc Cosh}(\zeta)\}$	$\{2\log(\varepsilon/4)\}^{-1}$
DNI	$\beta \to \infty$	$-(\beta/2\pi)\,\delta(\xi)$ $-(\varepsilon/\pi^2)\log(\beta)\xi(1-\xi^2)^{-1/2}$	$1 + \pi^{-1}(\varepsilon\zeta)\log(\varepsilon\zeta)$ $-(\varepsilon/\pi)\log(\beta)(\zeta^2-1)^{1/2}$	$-(\beta/2\pi)$

* Terms with real parts which are negligible compared to those retained have been omitted.

** Note that $\text{Re}\{\Gamma(\beta)\}$ is asymptotic to $-(2\pi/\beta)$ as $\beta \to \infty$.

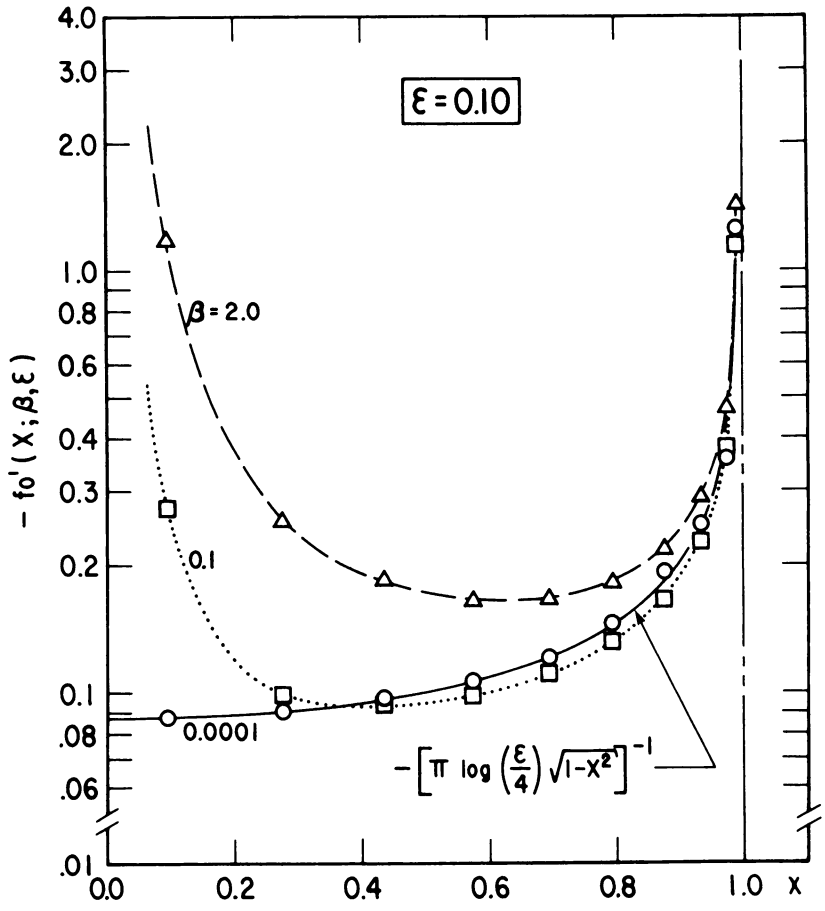

FIG. 3. Numerical approximations to the source density for the narrow deep inclusion. The solid line is the exact solution for $\beta = 0$.

value. The primary feature of this investigation is the introduction of a Green's function

$$G_1(z, z'; \beta) = \log\{(z - z')(z - z'^*)\} + 2\,Expei\{(z + z'^*)/\beta\}$$

which greatly facilitates both asymptotic analysis and numerical computation. To the best of the author's knowledge the simple closed-form singular solutions presented in the third section, Eqs. (8) and (11a), have not been published previously. The outer field—that is, the solution at points not too close to the disturbing inclusion—is characterized explicitly by Eqs. (18) and (19). The multiplicative factor $q(\beta, \epsilon)$ depends on the surface layer stiffness and the size and shape of the inclusion. The form of this factor was investigated for two extreme shapes of inclusion—a shallow wide inclusion and a deep narrow inclusion—and both the relation between the inner field (near the inclusion) and the outer field and the singularities of the inner field are worked out in detail. It is easy to show that for small inclusions $q(\beta, \epsilon)$ approaches

$$-(1/2\pi)\left[\int_C (\partial u/\partial n)\,ds + \beta\{(\partial u/\partial y)_1 - (\partial u/\partial y)_2\}\right],$$

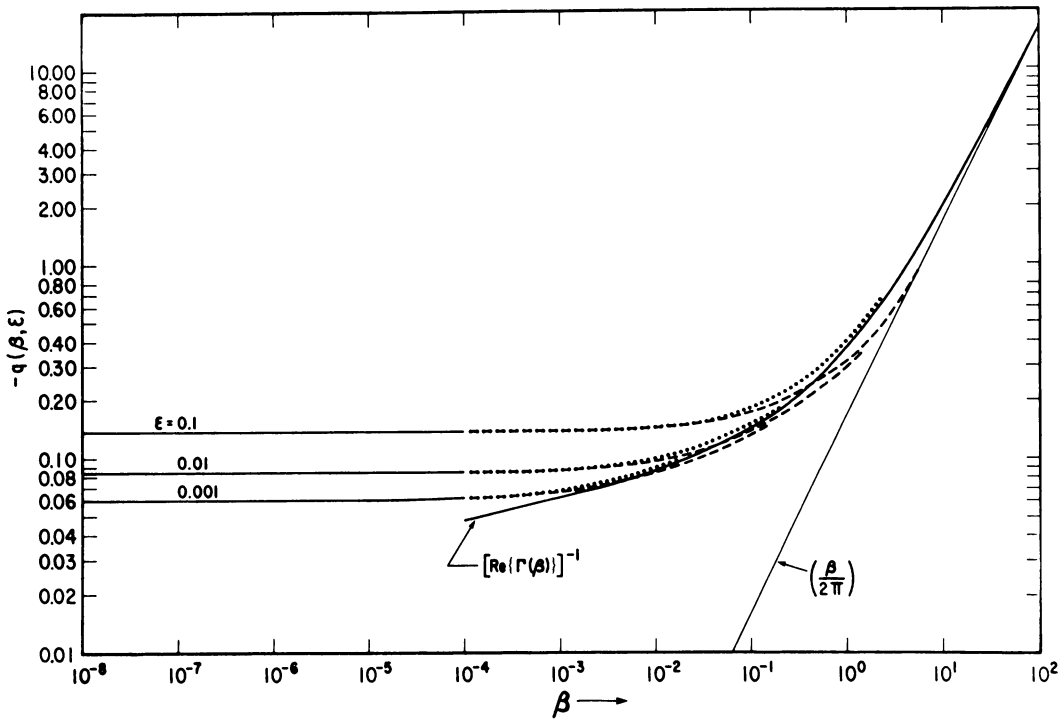

FIG. 4. Outer field strength factor as a function of β for several values of constant ϵ (dots = SWI, dashes = DNI).

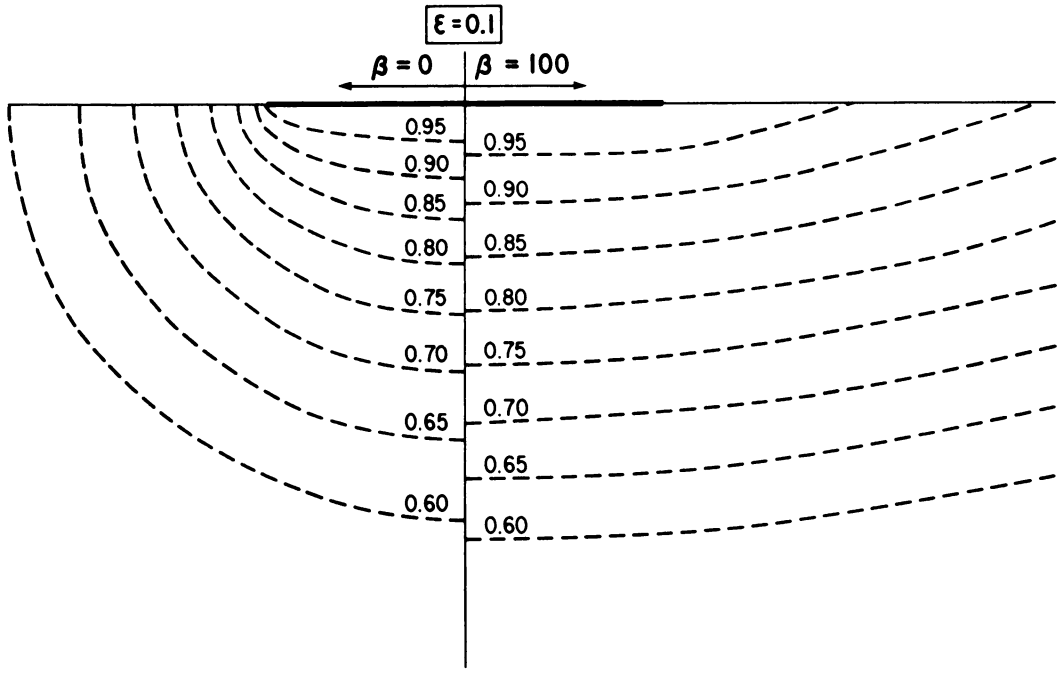

FIG. 5. Equipotentials (level curves of $u(x, y)$ = const.) near the shallow, wide inclusion for low and high surface stiffness.

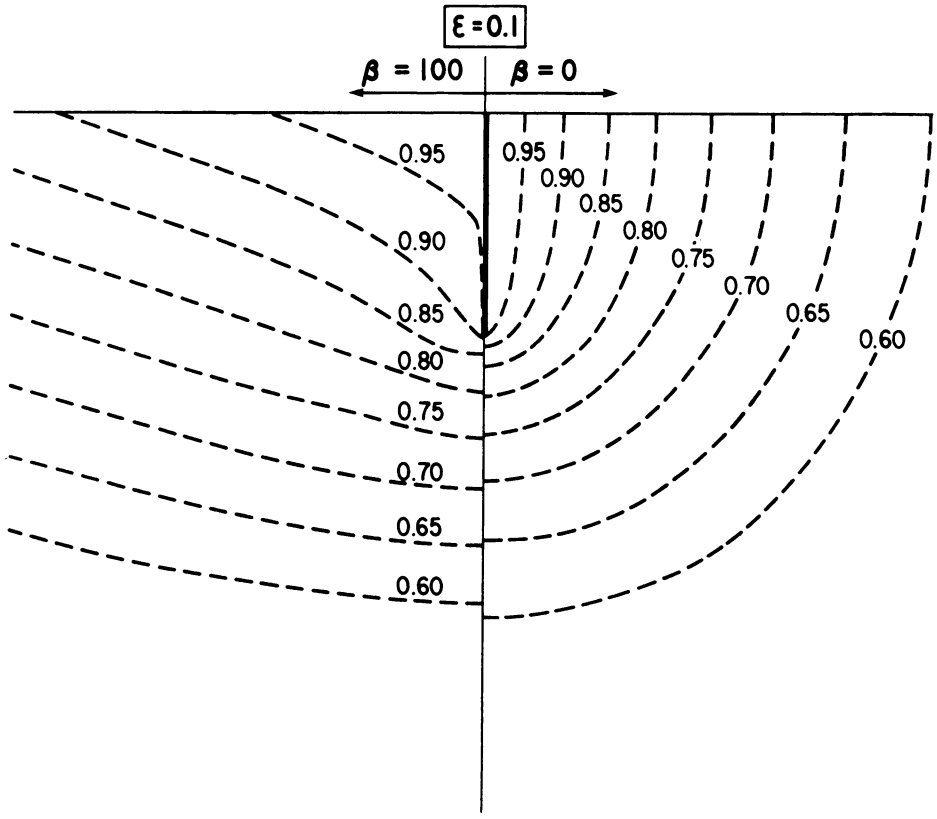

FIG. 6. Equipotentials (level curves of $u(x, y)$ = const.) near the deep, narrow inclusion for low and high surface stiffness.

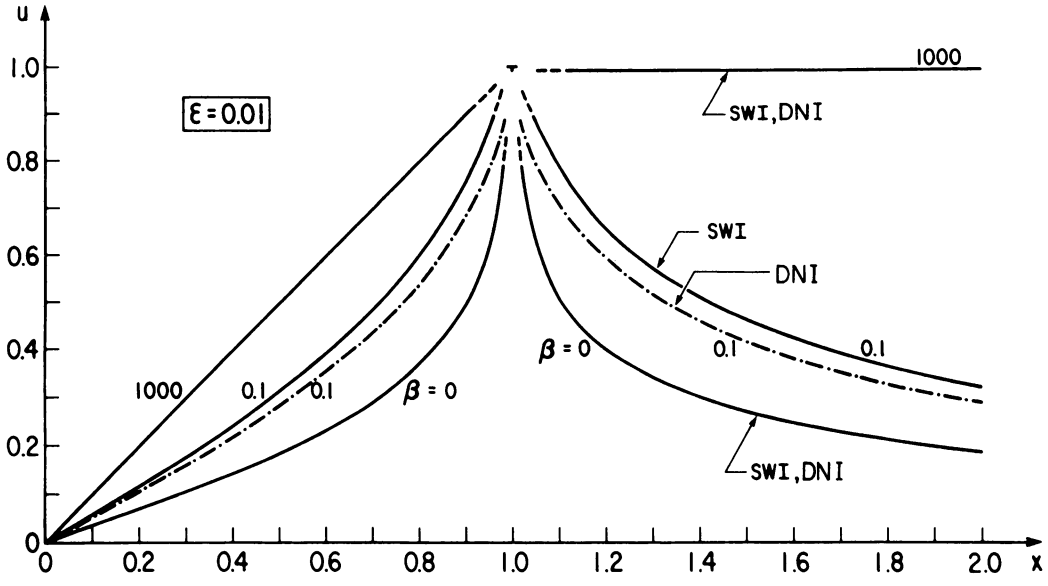

FIG. 7. Variation of $u(x, y)$ at the surface $x = 0$ as a function of surface stiffness.

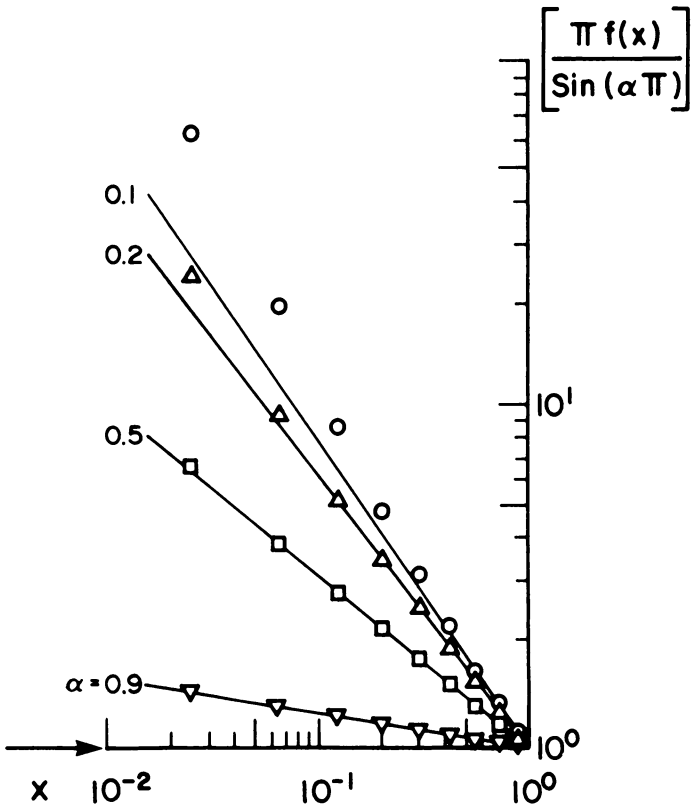

FIG. 8. Test of numerical scheme on Abel's equation. Solid lines represent exact solutions and symbols represent numerical approximations.

where the n is the normal direction into the inclusion and the subscripts 1 and 2 refer to the two points of intersection of the inclusion boundary with $x = 0$. Thus q, the integral of the source density over the boundary of the inclusion, can be interpreted as a physical quantity of primary importance: in the viscous flow and elastic antiplane-strain problems it is proportional to the total force acting on the inclusion (the sum of the contributions from the substrate and surface layer), whereas in the heat and electrical conduction problems it is proportional to the total flux of heat or charge out of the inclusion.

An examination of Fig. 4 shows that the outer field becomes independent of the stiffness parameter β if this parameter becomes either large or small. This has important consequences in surface viscometry [1], as it indicates that extremes of low and high surface viscosity cannot be measured from observations of surface velocity. In spite of the fact that Fig. 4 displays the behavior of $q(\beta, \epsilon)$ for the two extreme inclusion shapes only, these curves can be assumed to describe at least qualitatively the character of the outer field for an inclusion of any arbitrary shape. Thus it is always possible to choose the characteristic dimension ϵ for a small inclusion of prescribed shape so that $q(\beta, \epsilon)$ approaches 2 log $(\epsilon/4)$ as $\beta \to 0$: in fact, our analysis shows that in the limit of vanishing boundary stiffness the outer field strength $q(\beta, \epsilon) = \{\log(\epsilon^2)\}^{-1} + \cdots$ for an inclusion of any shape if ϵ is sufficiently small. Conversely, as the stiffness $\beta \to \infty$ we can expect on physical grounds that for an inclusion of any shape the outer solution at the surface will approach the (linear/constant) variation shown in Fig. 7 for $\beta = 1000$, and this in turn requires that $q(\beta, \epsilon)$ ap-

proach $-(\beta/2\pi)$ as shown in Fig. 4. No radical deviations from the curves of Fig. 4 are expected in the intermediate stiffness range for more general inclusion shapes.

One of the more interesting results of this investigation is the behavior of the singularities of the tips of the shallow and deep inclusions as the stiffness of the surface layer varies. For the narrow, deep inclusion the singularity of the tip is of the form $A(\zeta - 1)^{1/2}$ for all values of β. The strength of the singularity A increases with ϵ as $(\log(\epsilon))^{-1}$ for small values of β, and increases with both β and ϵ as $\epsilon \log(\beta)$ for large values of β. On the other hand, the tip singularity, say at $z = i$, for the shallow wide inclusion actually changes character as the stiffness increases. For small β this singularity is similar to that of the deep, narrow inclusion, namely of the form $A(\zeta - i)^{1/2}$ with A varying as $(\log(\epsilon))^{-1}$, but at high values of β the tip singularity assumes the weaker form $B(\zeta - i)\log(\zeta - i)$ with B proportional to ϵ and independent of β. It would be interesting to trace this transition in detail, but this has not been carried out in the present investigation. The variation of the tip singularities with surface stiffness should be of some interest in Mode III problems of linear elastic fracture mechanics [6] involving sharp inclusions in bodies with stiffened or bonded surfaces. However, it would be more pertinent for fracture mechanics applications to repeat the analysis employing the dislocation solution Eq. (11a), rather than the source solution Eq. (8), to synthesize cracks in bodies with surface layers.

The analysis presented in this paper exhibits clearly the connection between the inner field and the outer field via the source density function. Thus the source density is determined by solving an integral equation in the inner field, and the integral of the source density over the inclusion boundary is $q(\beta, \epsilon)$ which determines the strength of the outer field. The numerical calculations needed to fill in the curves of Fig. 4 for intermediate values of β were performed on a small computer. Undoubtedly it would be possible to improve the accuracy of the numerical approximations to the source density functions by repeating the calculations on a larger machine with increased precision, but as it is the integral of the source density rather than the source density itself which is of primary concern in this investigation, and as test cases have shown that our algorithm evaluates this integral with more than adequate accuracy, refinements in the numerical calculations were not considered necessary.

Conclusions. Simple closed-form solutions representing source and dislocation singularities have been derived for Laplace's equation in the half-plane, subject to a surface boundary condition of the form $\beta(\partial^2 u/\partial y^2) + (\partial u/\partial x) = 0$ on $x = 0$ for arbitrary values of the surface stiffness parameter β. The source solution is used to investigate the fields $u(x, y)$ generated by a small (characteristic dimension $= \epsilon$) inclusion of arbitrary shape on which u assumes a constant value, in the presence of a boundary on which u vanishes. Explicit formulas are presented for the outer field (not close to the inclusion). The outer field becomes independent of the surface stiffness as the latter approaches zero or infinity. Detailed analyses are carried out for two extreme shapes of inclusion—a shallow wide inclusion on the surface and a deep narrow inclusion penetrating below the surface. In these two cases analytic expressions for the inner field near the inclusion are derived for both high and low surface stiffness. For the deep narrow inclusion the tip singularity has a square-root character for all values of surface stiffness, with a strength that varies as $(\log(\epsilon))^{-1}$ at low and $\epsilon \log(\beta)$ at high surface stiffness. On the other hand, the tip singularity for the shallow wide inclusion changes character from a square-root singularity, with strength proportional to $(\log(\epsilon))^{-1}$ at low surface stiffness, to a logarithmic singularity with strength proportional to ϵ at high values of the surface stiffness.

Appendix: Numerical solution of the integral equation for the source density. When the parameter β is neither large nor small the integral equation for f_0', Eq. (24), can be solved numerically by the following scheme. Divide the integration contour C into N intervals by the introduction of $N+1$ mesh points $\zeta_0', \zeta_1', \cdots \zeta_N'$, where ζ_0' and ζ_N' coincide with the end points of C. Approximate f_0' by a constant value $(f_0')_m$ on the mth interval so that Eq. (24) can be approximated as

$$\sum_{m=1}^{N} (f_0')_m \mathrm{Re}\left\{\int_{C_m} G'(\zeta, \zeta'; \beta, \epsilon)\, e^{-i\phi} d\zeta'\right\} = 1, \tag{A1}$$

where C_m represents the arc between ζ_m' and ζ_{m-1}'. We require that this equation be satisfied at N discrete values of ζ, $\{\zeta_n\}$, where ζ_n lies in the nth interval and may for convenience be chosen as the midpoint of that interval. If C is smooth and the number of mesh points is large we may approximate ϕ by its value ϕ_n at ζ_n, so that a discrete numerical approximation to f_0' can be found by solving the system of simultaneous algebraic equations

$$\sum_{m=1}^{N} A_{nm}(f_0')_m = 1, \qquad n = 1, 2, \cdots, N \tag{A2}$$

where

$$A_{nm} = \mathrm{Re}\left\{e^{-i\phi_n} \int_{\zeta_{m-1}'}^{\zeta_m'} G; (\zeta_n, \zeta'; \beta, \epsilon)\, d\zeta'\right\}. \tag{A3}$$

For the SWI the integral appearing in Eq. (A3) is evaluated explicitly as

$$\int G'(\zeta, \zeta') d\zeta' = -2(\zeta - \zeta')\{\log(\zeta - \zeta') - 1\} - 2\left(\frac{\beta}{\epsilon}\right)\{\log(\zeta - \zeta') + Expei[(\zeta - \zeta')/(\beta/\epsilon)]\} + 2\{\log(\epsilon) - \log(2i) - Expei(2i/\beta)\}\zeta' \tag{A4}$$

whereas for the NDI the corresponding integral is

$$\int G'(\zeta, \zeta')\, d\zeta' = (\zeta + \zeta')\{\log(\zeta + \zeta') - 1\} - (\zeta - \zeta')\{\log(\zeta - \zeta') - 1\} + 2\left(\frac{\beta}{\epsilon}\right)\{\log[(\zeta + \zeta')/(\beta/\epsilon)] + Expei[(\zeta + \zeta')/(\beta/\epsilon)]\} + 2\{\log(\epsilon) - \log(2i) - Expei(2i/\beta)\}\zeta'. \tag{A5}$$

Thus the coefficients of Eqs. (A2) can be easily evaluated by a digital computer.

To gauge its accuracy this algorithm was tested on a simple Abel equation of the form

$$\int_0^1 \frac{H(x - \xi)}{(x - \xi)^\alpha} f(\xi)\, d\xi = 1, \qquad 0 < \alpha < 1 \tag{A6}$$

where H is the step function. The solution of this equation is

$$f(x) = \{(\sin(\alpha\pi))/\pi\}\, x^{\alpha - 1} \tag{A7}$$

and the coefficients, Eqs. (A3), in this case are simply

$$\begin{aligned} A_{nm} &= [(x_n - \xi_{m-1})^{1-\alpha} - (x_n - \xi_m)^{1-\alpha}]/(1-\alpha) \quad \text{for} \quad n > m, \\ &= [(x_n - \xi_{n-1})^{1-\alpha}]/(1-\alpha) \quad \text{for} \quad n = m, \\ &= 0 \quad \text{for } n < m. \end{aligned} \tag{A8}$$

The numerical solution was computed for several numbers and spacings of the mesh points $\{\xi_n\}$. Generally the computed values of f agreed reasonably well with the exact solution, Eq. (A7), except in the immediate vicinity of the singular point $x = 0$, so long as α was not close to zero. As α approached zero the algorithm became unstable and numerical oscillations appeared, but this was to be expected since then the solution approaches a δ-function at the origin and such behavior must eventually frustrate any numerical scheme. The performance of the algorithm could be improved at low values of α by increasing the number of mesh points and/or by averaging the computed values over several adjacent mesh points. Representative results are shown in Fig. 8. These results were computed using a total of forty mesh points with a mesh point density which increased toward the singular point, and averaging the computed values over four adjacent points. The numerical approximations to f are seen to be quite good even with this relatively crude mesh, except near the singular point for $\alpha = 0.1$. The algorithm gave the integral of f over the interval (0, 1) correctly to within 0.01% for all the cases shown: the integral of the source density function is a quantity of primary interest as it determines the outer field through Eq. (19).

The scheme outlined above was used to compute numerical approximations to the source density functions, such as those shown in Fig. 3, and the integrals of those functions $q(\beta, \epsilon)$, shown in Fig. 4 for intermediate values of β. The computations were carried out on a PDP-11/15 minicomputer with a 16K-word memory using a total of forty mesh points. The mesh point density was chosen to increase toward the tips of the inclusions, which are singular points for all values of β, and the computed results were smoothed by averaging over four adjacent mesh points.

References

[1] F. C. Goodrich, *The hydrodynamical theory of surface shear viscosity*, Prog. Surf. Memb. Sci. 7, 151–181 (1973)

[2] D. A. Simons, *Scattering of a Love wave by the edge of a thin surface layer*, J. Appl. Mech. **(4) 42,** 842–846 (1975)

[3] R. J. Mannheimer and R. A. Burton, *A theoretical estimation of the viscous-interaction effects with a torsional (knife-edge) surface viscometer*, J. Coll. Int. Sci. **(1) 32,** 73–80 (1970)

[4] F. C. Goodrich and L. H. Allen, *The theory of absolute surface shear viscosity, part V. The effect of finite ring thickness*, J. Coll. Int. Sci. **(3) 40,** 329–336 (1972).

[5] M. Abramowitz and J. Stegun, eds., *Handbook of mathematical functions*, National Bureau of Standards, Washington, 1965, p. 228

[6] J. R. Rice, *Mathematical analysis in the mechanics of fracture* in *Fracture*, vol. 2 (H. Liebowitz, ed.), Academic Press, New York, 1968, p. 191

[7] M. VanDyke, *Perturbation methods in fluid mechanics*, Parabolic Press, Stanford, 1975, p. 77

[8] G. F. Carrier, M. Krook, and C. E. Pearson, *Functions of a complex variable*, McGraw-Hill, New York, 1966, p. 428